DTU Library

Composite Films of Arabinoxylan and Fibrous Sepiolite: Morphological, Mechanical, and Barrier Properties

Sárossy, Zsuzsa ; Blomfeldt, J.O.; Hedenqvist, Mikael S. ; Bender Koch, Christian ; Sinha Ray, Suprakas ; Plackett, David

Link back to DTU Orbit

Composite Films of Arabinoxylan and Fibrous Sepiolite: Morphological, Mechanical, and Barrier Properties

Zsuzsa Sárossy,[†] Thomas O. J. Blomfeldt,[‡] Mikael S. Hedenqvist,[‡] Christian Bender Koch,[§] Suprakas Sinha Ray,[⊥] and David Plackett*,[†]

[†]Department of Chemical and Biochemical Engineering, Technical University of Denmark, DK-2800 Kgs. Lyngby, Denmark

[‡]Department of Fibre and Polymer Technology, KTH Royal Institute of Technology, SE-100 44 Stockholm, Sweden

[§]Department of Chemistry, University of Copenhagen, Thorvaldsensvej 40, DK-1871 Frederiksberg C, Denmark

[⊥]DST/CSIR Nanotechnology Innovation Centre, National Centre for Nano-Structured Materials, Council for Scientific and Industrial Research, P.O. Box 395, Pretoria 0001, Republic of South Africa

ABSTRACT: Hemicelluloses represent a largely unutilized resource for future bioderived films in packaging and other applications. However, improvement of film properties is needed in order to transfer this potential into reality. In this context, sepiolite, a fibrous clay, was investigated as an additive to enhance the properties of rye flour arabinoxylan. Composite films cast from arabinoxylan solutions and sepiolite suspensions in water were transparent or semitransparent at additive loadings in the 2.5–10 wt % range. Scanning electron

microscopy showed that the sepiolite was well dispersed in the arabinoxylan films and sepiolite fiber aggregation was not found. FT-IR spectroscopy provided some evidence for hydrogen bonding between sepiolite and arabinoxylan. Consistent with these findings, mechanical testing showed increases in film stiffness and strength with sepiolite addition and the effect of poly(ethylene glycol) methyl ether (mPEG) plasticizer addition. Incorporation of sepiolite did not significantly influence the thermal degradation or the gas barrier properties of arabinoxylan films, which is likely a consequence of sepiolite fiber morphology. In summary, sepiolite was shown to have potential as an additive to obtain stronger hemicellulose films although other approaches, possibly in combination with the use of sepiolite, would be needed if enhanced film barrier properties are required for specific applications.

KEYWORDS: arabinoxylan, sepiolite, composite film, mPEG, tensile properties, barrier properties
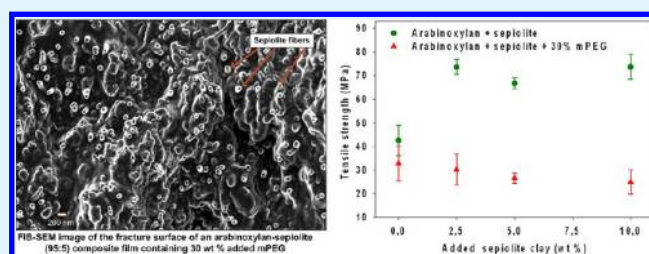
■ INTRODUCTION

Plant polysaccharides derived as byproducts from agricultural processes have lately received much attention as substrates for potential future packaging materials.[1−4] Xylan-type hemicelluloses are the most abundant heteropolysaccharides in agricultural residues and there has been increasing interest in their use in food packaging and other applications.[5] Indeed, over the past few years, there have been a number of reports discussing films prepared from xylans extracted from aspen or beech, barley husks, oat spelts, wheat bran, rye grains, or corn hulls and bran.[1−3,6,7] Agricultural byproducts such as oat spelt or barley husk arabinoxylans have been shown to provide good oxygen and/or grease barrier films in applications where moderately high water vapor permeability is required.[1,2] Hemicelluloses are hydrophilic polysaccharides and films tend to show poor properties in highly humid environments,and, on the application, mechanical properties may also need improvement. For these reasons, research on new and improved hemicellulose films continues to be reported.[3,8−10]

A potential route to improving mechanical and barrier properties is the addition of nanofillers to form hemicellulose-based nanocomposites. In comparison to unmodified polymers,

the characteristic features of nanocomposites generally include higher modulus, increased strength, decreased gas permeability and increased thermal stability. These effects are in large part due to the high surface area of the well-distributed nanoparticles and the resulting increased interfacial area.[11−13] Clay-biopolymer nanocomposites are of particular interest because of the significant potential to improve material properties; however, in the case of hemicelluloses, the number of publications discussing the effects of clay nanofiller addition remains quite limited.[13,14] Xylan-clay films have been made focusing on the use of layered silicate clays such as montmorillonite (MMT). For example, Ünlü et al. [14] prepared films using corn cob xylan and MMT. Their research using electrokinetic, rheological and crystallinity measurements suggested that interactions took place on the MMT surface and that the xylans were not oriented into the MMT interlayer spaces.
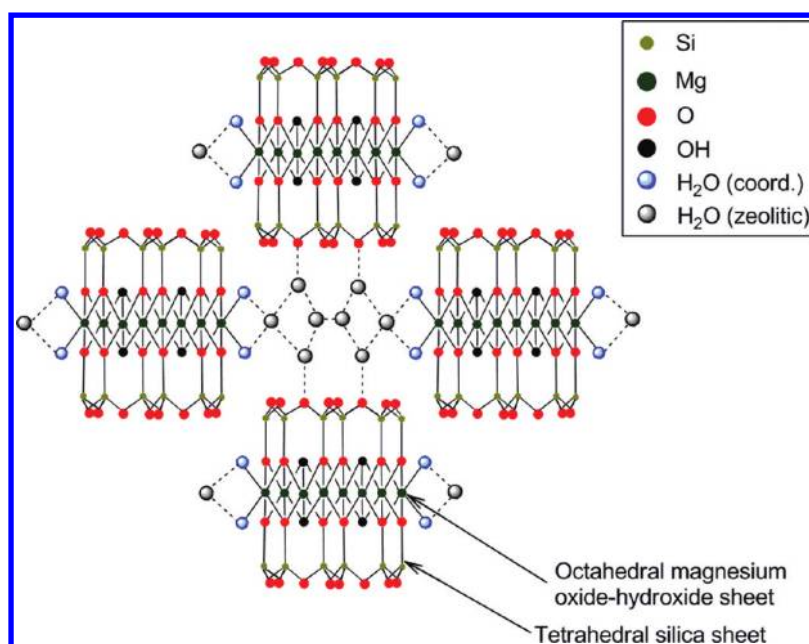
Figure 1. Transection of the sepiolite structure. Adapted from ref 24.

In addition to the use of MMT, the interesting potential of other clays having tubular or fibrous morphologies has been recognized. In the case of sepiolite, a fibrous clay, researchers have investigated its use as a filler in natural rubber and plastics such as poly(vinyl chloride).[15] Combinations of sepiolite with biopolymers such as starch, chitosan, gelatin, and polylactide have also been investigated.[12,16−18] As one example, biocompatible biomaterials were prepared with collagen and sepiolite and used as gel-like complexes.[19] Improved mechanical properties were found in these sepiolite/biopolymer nanocomposites, which is in general comparable with the improvements obtained with other fiber-like nanofillers (e.g., cellulose whiskers). Chivrac et al.[12] studied the effects of sepiolite addition on the mechanical properties of starch nanocomposites. In their study a comparison was made between sepiolite and other fibrous fillers, such as cellulose whiskers or cellulose nanofibers, as well as hectorite, a layered nanoclay. Evidence for strong hydrogen bonding was noted at cellulose whisker loadings above the percolation threshold. Reinforcing effects were observed when either cellulose whiskers or cellulose nanofibers were used and in both cases mechanical property improvements were similar to those achieved when using a layered or fibrous clay additive. In these composites, the Young's modulus increased and there was no effect on the strain at break. When fibrous sepiolite and MMT were compared, it was found that sepiolite increased the Young's modulus and tensile strength to a greater extent than MMT, presumably due to the morphology of the clay, the increased crystallinity of the nanocomposites and interaction between the starch matrix and sepiolite.

Sepiolite has a hydrated magnesium silicate composition with a theoretical unit-cell formula equivalent to $Si_{12}O_{30}Mg_8(OH)_4 \cdot (H_2O)_4 \cdot 8H_2O$. Alternating longitudinal blocks and channels (tunnels) are found in the sepiolite structure, producing long needles with a high surface area (approximately 374 m^2/g).[11] The blocks are built up of two layers of tetrahedral silica, sandwiching an octahedral magnesium oxide-hydroxide layer in the center (Figure 1). The composite layers are off-set, hence allowing the formation

of tunnel-like micropores (channels), running parallel to the fiber axis. The channels in the sepiolite structure are occupied by water coordinated to the magnesium ions at the edges of the octahedral layers and zeolitic water associated with the clay structure by hydrogen bonding inside the tunnels. Silanol (Si-OH) groups appear at the external surface edges of the sepiolite structure.[12,20−22] The numerous silanol groups provide sites for hydrogen bonding and Van der Waals interactions in composites, contributing to the reinforcing effect of sepiolite. From this perspective, the availability of silanol groups for hydrogen bonding with other moieties mostly occurs at the edges. Sepiolite has a microfibrous morphology with fiber lengths of 2−10 μm and diameters in the range of 2−100 nm,[17,23] pointing to aspect ratios of 20−200.

We focused our work on composite films using arabinoxylan from rye grains and sepiolite at loadings between 2.5 and 10 wt %. The objective was to observe potential improvements in the mechanical and barrier properties of arabinoxylan films. Morphology, crystallinity and structural changes in the composite films were studied as well as tensile and barrier properties and these characteristics were compared with those of unreinforced arabinoxylan films. To the best of our knowledge, this is the first report on the production and mechanical/barrier properties of sepiolite-hemicellulose composite films.

■ MATERIALS AND METHODS

Materials. Arabinoxylan (Lot 20601) from rye flour (RAX) was purchased from Megazyme International Ireland Ltd. (Bray, Ireland). The arabinoxylan was a high-viscosity sample with reported Ara/Xyl ratio of 0.64, purity ∼90% and ash content of 4.5 wt %. Poly(ethylene glycol) methyl ether (mPEG) and sepiolite were purchased from Sigma-Aldrich (Steinheim, Germany). The sepiolite powder from Aldrich has a unit cell formula of $Mg_2H_2Si_3O_9 \cdot xH_2O$ and a reported Mg content of approximately 13%.

Film Casting. Neat RAX and RAX-sepiolite composite films containing the two components in ratios 97.5:2.5, 95:5, 90:10, and 80:20 were prepared, although the last of these, containing 20 wt % sepiolite, was prepared only for tests on light transmission. RAX was mixed into MilliQ water for 4 h at 70 °C under magnetic stirring at a
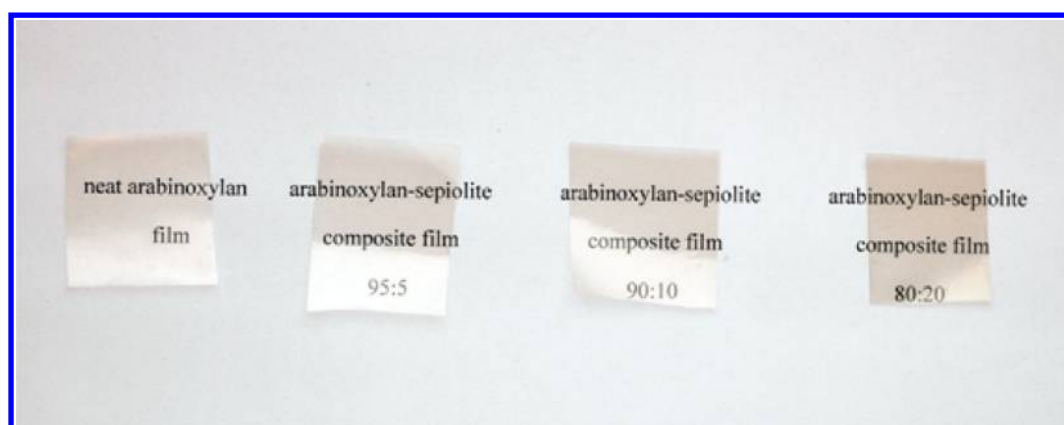
Figure 2. Images of neat rye arabinoxylan (RAX) and rye arabinoxylan (RAX)-sepiolite composite films, from left to right, RAX, RAX-sepiolite 95:5, 90:10, and 80:20. Films were placed on a white paper sheet with printed text.

concentration of 10 g/L. Sepiolite suspensions were prepared at a concentration of 2.5 g/L in MilliQ water and were sonicated for one hour under magnetic stirring using a UP 400 S ultrasonic processor with a 22 mm diameter tip and a maximum amplitude of 100 μm at 25% output (Hielscher Ultrasonics GmbH, Teltow, Germany). The sepiolite suspension and RAX solution were then mixed in appropriate ratios using magnetic stirring. The mixtures were degassed by ultrasonication for 15 min and suitable volumes poured into Teflon-coated Petri dishes for the purpose of film casting. In selected cases, mPEG plasticizer was added to the mixed RAX-sepiolite formulations prior to ultrasonication at 30 wt % loading on the basis of total RAX-sepiolite weight. mPEG was chosen as the plasticizer as it is nontoxic and may be applied in foods, cosmetics or pharmaceuticals.[25] mPEG has not to our knowledge been used as a plasticizer in previous studies on hemicellulose films. Films were prepared by drying the contents of the Petri dishes at 23 °C and 50% relative humidity (RH) and held under these conditions for at least four days before analysis. The thickness of the films was measured at 10 points using a Mega-Check Pocket Coating Thickness Meter with micrometer precision (List-Magnetik, Leinfelden-Echterdingen, Germany) and average film thicknesses were calculated.

Light Transmittance. The light transmittance of the films was measured for two replicates of each film type over the 190−890 nm wavelength range with an Ultrospec 2100 pro UV−visible spectrophotometer (Biochrom Ltd., Cambridge, UK). The light transmittance was normalized to a thickness of 30 μm for all tested films. Film opacity, normalized to a film thickness of 30 μm and expressed as absorbance × nanometers, was calculated with an integration procedure as similarly reported by Siró et al.[26]

Fourier Transform Infrared (FT-IR) Spectroscopy. FT-IR spectra were collected using a Perkin-Elmer Spectrum One spectrometer (PerkinElmer Life and Analytical Sciences, Shelton, WA, USA). For this purpose, the film samples were tested using an STI Thunderdome attenuated total reflectance (ATR) attachment. Sepiolite powder samples were pressed into KBr pellets (2 mg sample/ 200 mg KBr). Spectra were obtained based on 16 scans collected in the range 400−4000 cm^{-1} at a resolution of 2 cm^{-1}.

X-ray Diffraction. X-ray diffraction was used to study structural changes in RAX-sepiolite composite films in comparison to neat RAX film and sepiolite powder. A Siemens D5000 X-ray diffractometer (Siemens Analytical and X-Ray Instruments Inc., Madison, WI, USA) equipped with a Co (λ = 0.179 nm) tube and a diffracted beam monochromator was used. Diffractograms were collected in the 2Θ range of 3−30° using a step size of 0.05° and a counting time of 20 s. One film sample was tested from each cast film type.

Microscopy. The fracture surface morphology of the composites after tensile testing was studied using focused ion beam scanning electron microscopy (FIB-SEM) on an AURIGA CrossBeamWork-station (Carl Zeiss, Oberkochen, Germany). The samples were sputter-coated with carbon in a vacuum chamber before examination.

The chemical composition of the composites was analyzed with energy-dispersive X-ray spectroscopy (EDX, NORAN System Six, Thermo Scientific, Waltham, MA) in a JEOL 7500F SEM (JEOL Ltd., Tokyo, Japan).

Thermogravimetric Analysis (TGA). The thermal degradation of films and sepiolite powder was studied under N$_2$ atmosphere at a flow rate of 30 mL/min using a Netzsch TG 209 F3 Tarsus thermogravimetric analyzer (NETZSCH-Gerätebau GmbH, Selb, Germany). The weight of the analyzed film pieces varied between 1 and 2 mg and alumina pans were used for the measurements. The samples were heated from 36 to 900 °C at a rate of 20 °C/min, including an isothermal ramp at 120 °C for three minutes.

Tensile Testing. Tensile testing was performed on rectangular film samples (10 mm x 80 mm) using an Instron 5944 universal testing machine (Instron Corp., High Wycombe, England) with Instron grips series nr. 2712−019, according to the ASTM standard test method D882−09.[27] Film test samples were cut using a Synrad 48−5 laser cutter (Synrad, Mukilteo, WA, USA). Sample testing was performed in a conditioned room at 23 ± 1 °C and 50 ± 2% RH. A load cell of 50 N was used with an extension rate of 5 mm/min and an initial grip distance of 50 mm. A preload of 0.1 N (extension rate = 5 mm/min) was applied to ensure measurement of straight samples. Ten specimens were tested from each sample, which were conditioned at 23 °C and 50% RH for 120 h before testing.

Statistical analyses were performed on the tensile test results using Tukey-Kramer HSD (Honestly Significant Difference) tests on data from ten specimens and the statistical software JMP version 5.0.1 (SAS Institute Inc., Cary, NC, USA) at a significance level of 0.05.

Water Vapor Permeability. The water vapor permeability was measured for three films per sample type according to the ASTM 96/E 96 M − 05 standard.[28] Films were sealed to aluminum cups, containing 21 g dry CaCl$_2$ as a desiccant. This setup included an air gap of 6 mm between the desiccant and the underside of the film. The aluminum cups were placed into a climate chamber with controlled relative humidity and temperature (50% RH and 23 °C). The cups were weighed 8−10 times over the period of three days. Calculations were performed according to the method of Mikkonen et al.[29] The water vapor transmission rate (WVTR) was calculated from the linear regression of the slope of weight gain vs time by dividing the slope by the test cell mouth area. The water vapor permeability (WVP) was obtained by multiplying the WVTR by the thickness of the film and dividing it by the water vapor partial pressure difference between the two sides of the film. The correction method of Gennadios et al.,[30] in which the air gap is taken into account, was used as a means of calculating the water vapor partial pressure at the underside of the film. However, data calculated using this correction method gave WVP values which were not significantly different from those calculated without correction.

Oxygen Permeability. The oxygen transmission rate (OTR) of films was measured with an OPT-5000 Oxygen Permeability Tester

3380

dx.doi.org/10.1021/am3002956 | ACS Appl. Mater. Interfaces 2012, 4, 3378−3386

(PBI-Dansensor A/S, Ringsted, Denmark) containing a ceramic solid-state oxygen sensor. Measurements were performed at 23 ± 0.03 °C and 50 ± 2% RH. The test samples were placed in a permeability chamber which consisted of an upper (feeding) and a bottom (receiving) chamber. Dry nitrogen containing less than 0.1 ppm oxygen (Alphagaz 2, Air—Liquide Danmark) was used as carrier gas and pure oxygen (N45, Air—Liquide Danmark) served as the test gas. Inlet pressure was set to four bars at the regulator. The oxygen permeability was calculated by multiplying the OTR with the thickness of the films and dividing with the pressure value of the measuring chamber. The oxygen permeability was determined for two replicates of each film type.

■ RESULTS AND DISCUSSION

Visual Properties and Light Transmittance. All cast films were cohesive and the thickness of the films varied between 25 and 45 μm. Light transmittance showed a general decrease with increasing clay content. All cast films were at least semitransparent; however, minor color changes were visible as the clay loading was increased to 10 and 20 wt %, as can be seen in Figure 2. The neat RAX films showed some slightly opaque spots, which may have been due to minor quantities of proteins precipitated during sample dissolution or lignin contamination. Significant contamination by lignin was not expected in the RAX since the material was alkali-extracted from rye grains and only minor amounts of aromatic components, such as ferulic acids, which would be characteristic of lignin, were found. Robertson et al.[31] measured the ferulic acid content of the RAX material used in this study at a level of 1.55 mg/g. The light transmittance of the films as a function of wavelength is shown in Figure 3. The neat RAX film and films
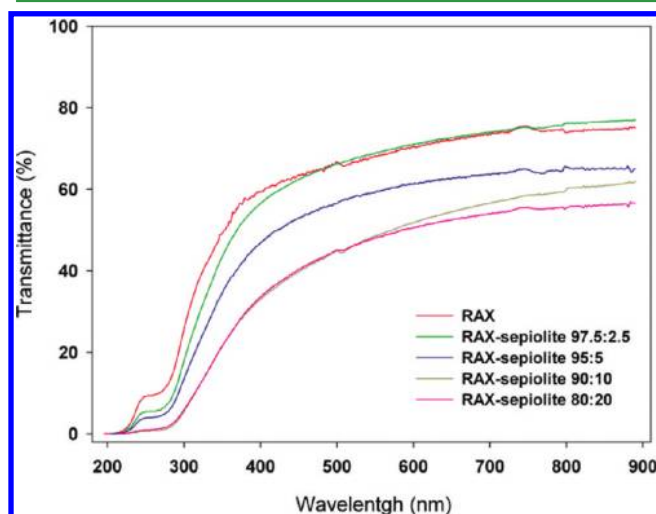

Figure 3. UV—vis transmittance of rye arabinoxylan (RAX) and RAX-sepiolite composite films.

containing lower amounts of sepiolite (2.5 and 5 wt %) showed a minor inflection in light transmission at 260 nm. This finding could be attributable to some aromatic compounds such as lignin or proteins absorbing in the ultraviolet region, because the typical absorption of aromatic compounds such as ferulic acid or aromatic amino acids occurs in the range 200—300 nm.[32] The film opacities were calculated and a good correlation was found with the visual appearance. The calculated values were 276.2, 217.3, 328.0, 349.2, 398.5 (AU × nm) for the RAX, RAX-sepiolite 97.5:2.5, 95:5, 90:10, and 80:20 films, respectively. These differences suggest that 5 wt % or higher

amounts of added clay were not well dispersed and therefore introduced some opacity.[33] This effect was particularly noticeable at 10 and 20 wt % sepiolite loadings.

Microscopy. The sepiolite distribution and the presence of clay aggregates was studied with FIB-SEM. Figure 4a shows the
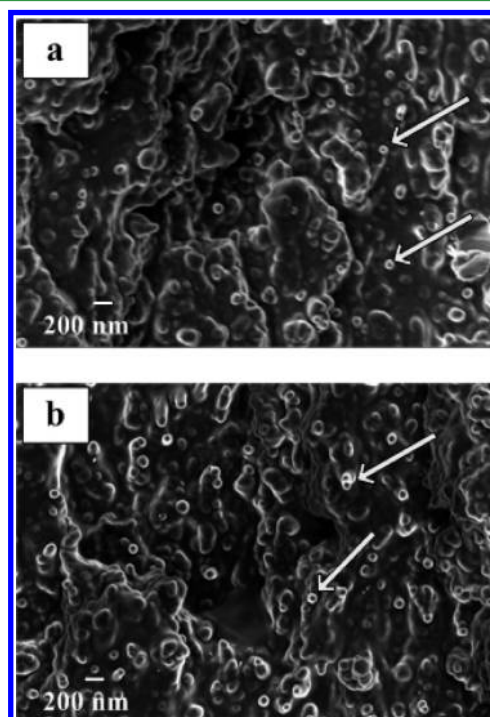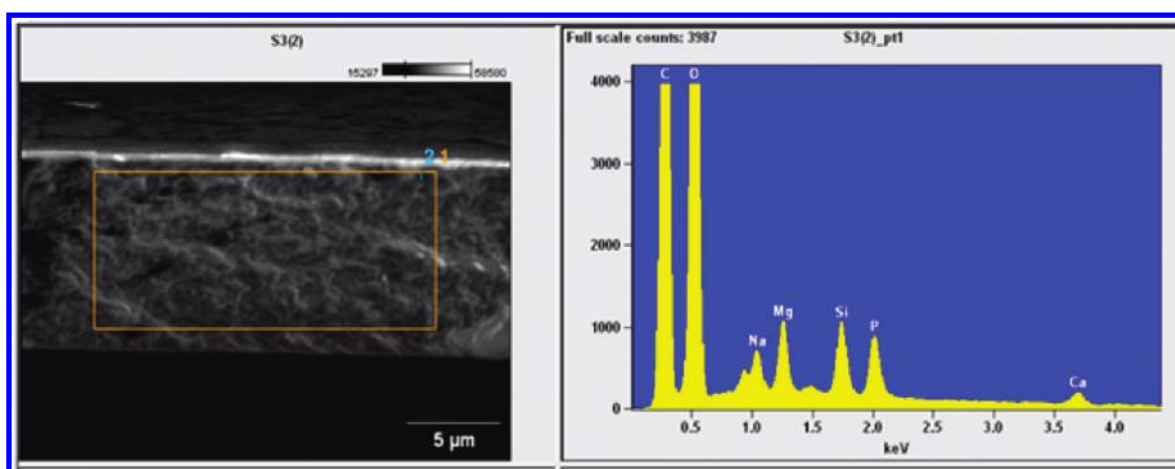

Figure 4. FIB-SEM images of rye arabinoxylan (RAX)-sepiolite composites, (a) RAX-sepiolite 97.5:2.5 and (b) RAX-sepiolite 95:5. Scale bar = 200 nm. The arrows point to sepiolite fibers (fiber diameter: 100—200 nm).

distribution of 2.5 wt % sepiolite in the RAX matrix in the cross-section of tensile-tested films and Figure 4b illustrates the composite film cross-section containing 5 wt % sepiolite after tensile testing. The images show well-dispersed sepiolite fibers with minimal pull-outs, indicating strong binding between the sepiolite and the RAX matrix. The lower level of clay addition is apparent from the fewer fibers visible in the image of the RAX-sepiolite 97.5:2.5 film (Figure 4a) which contains half the amount of sepiolite as the film RAX-sepiolite 95:5. The RAX matrix shows a nodular appearance and a similar morphology to that reported by Stevanic et al.[34] in a study on arabinoxylan-bacterial cellulose composite films based on the same RAX. From the FIB-SEM images, the diameter of the sepiolite fibers is estimated to be ~100 nm, which is comparable with values reported in an earlier study.[17]

The composition of the composite films was studied by energy-dispersive X-ray spectroscopy (EDX) (Figure 5). As expected, EDX analysis revealed the occurrence of silicon and magnesium in an approximate ratio of 1.5 to 1 (atomic ratio) due to the presence of sepiolite. Phosphorus and calcium, present in the pure RAX and dominating in the ash, were also detected in the films.

FT-IR Spectroscopy. FT-IR spectra of sepiolite powder, RAX, and RAX-sepiolite films were collected in order to examine the presence of clay in the RAX matrix as well as to study changes in molecular structure or the formation of new chemical bonds. The spectrum of neat RAX (Figure 6) shows a

Figure 5. Low-magnification SEM image and corresponding EDX spectrum for the cross-section of a 95:5 rye arabinoxylan (RAX)-sepiolite composite film.
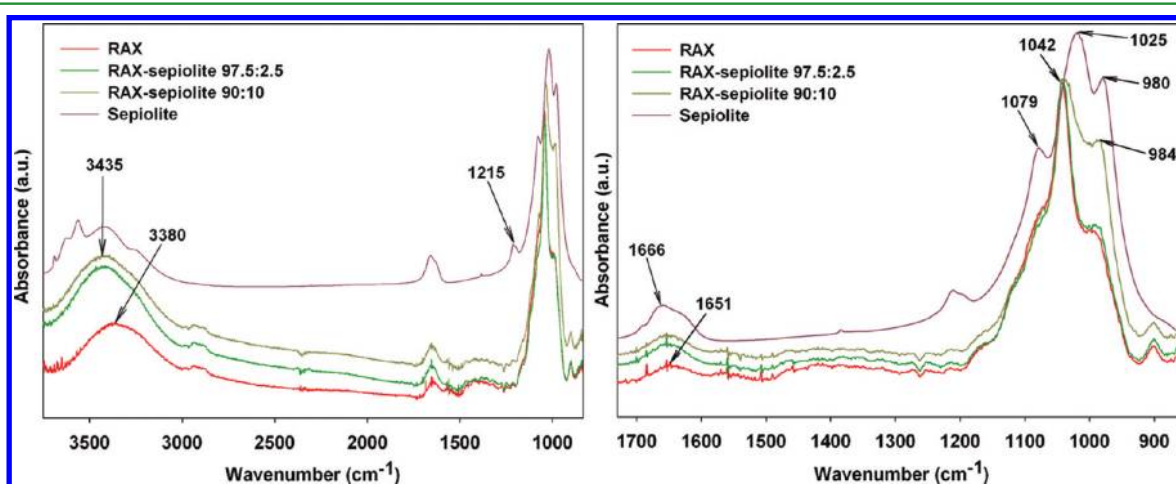
Figure 6. FT-IR spectra of sepiolite, neat rye arabinoxylan (RAX), and composites of RAX-sepiolite.

strong absorption band at 1042 cm^{-1}, which is due to C-OH bending.[35,36] A weak absorption band at 900 cm^{-1} is characteristic of β-(1→4) glycosidic linkages between the xylose units in the RAX structure. A low intensity amide I absorption band appears at approximately 1651 cm^{-1}, which is consistent with a low level of protein contamination.[37] The absence of an absorption band at 1517 cm^{-1} indicates that very little, if any, ferulic acid is present.

The FT-IR spectrum of sepiolite (Figure 6) shows peaks in the 3400−3650 cm^{-1} region attributed to OH stretching vibrations of zeolitic and Mg-coordinated water molecules occurring inside the tunnels and bound to the magnesium ions in the mineral structure. Bending vibrations of the zeolitic or channel water molecules contributed to a signal at 1666 cm^{-1}. Peaks associated with Si-O bonds in the tetrahedral sheets were seen between 1300 and 800 cm^{-1}. Si-O-Si bonds contributed to bands at 1215 and 1079 cm^{-1} and in-plane Si-O-Si vibrations were observed at ~1025 and 980 cm^{-1}.[16,38]

The spectra of RAX-sepiolite films show some differences when compared with the spectra of the pure components. The shoulder in the spectrum of RAX at 995 cm^{-1} grew with sepiolite addition and a peak appeared at 984 cm^{-1} in the spectrum of the RAX-sepiolite 90:10 film, which can be associated with the higher clay content of this film. A slight increase in the intensity of the peak at 1666 cm^{-1} was also

noticed; however, there is overlap here with the RAX amide I band, which hinders interpretation. A peak appearing at 3380 cm^{-1} in the spectrum of the RAX film shifted toward higher wavenumbers with addition of sepiolite, as was observed for example at 3435 cm^{-1} in the spectrum of the RAX-sepiolite 90:10 film. This shift of the OH stretching band is likely indicative of hydrogen-bonding interactions between RAX and sepiolite.

X-ray Diffraction. Arabinoxylans with a high degree of substitution (Ara/Xyl ratio of 0.5 or greater) are amorphous and show no distinct peaks in the X-ray diffraction pattern. Decreasing the arabinose substitution (Ara/Xyl ratios between 0.37 and 0.2) on the xylan main chain can lead to increasing crystallinity, showing distinct crystalline peaks between 4.9 and 3.3 Å.[3,39] It is believed that the unsubstituted regions of the chains crystallize while the more highly substituted regions of the xylan chains remain amorphous. The arabinoxylan (RAX) applied in this study was highly substituted (reported Ara/Xyl ratio of 0.64) and therefore the presence of a crystalline structure in the polymer was neither expected nor found. The neat RAX film exhibited a broad peak with a maximum at 4.5 Å (Figure 7A).

The characteristic (110) diffraction of sepiolite dominates the pattern of the pure sepiolite sample (Figure 7E), and in addition, an unidentified impurity can be detected with a *d*-
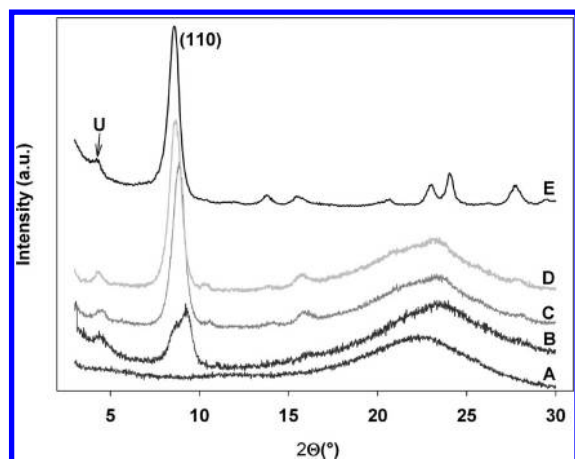
Figure 7. X-ray diffraction patterns of (A) neat rye arabinoxylan (RAX), (E) sepiolite and composite films of RAX-sepiolite, RAX-sepiolite (B) 97.5:2.5, (C) 95:5, and (D) 90:10. (110) indicates the position of the characteristic peak from sepiolite and U an unidentified mineral in the sepiolite sample.

spacing of 22.5 Å. A minor but distinct shift of the (110) diffraction can be observed in the composite films. This shift is caused by the off-set of the effective diffraction plane between the films and the shift scales with the effective density of the films. The maximum of the broad peak in the XRD pattern of the films is also shifted slightly toward higher angles (Figures 7A–D). This may signify a change in the polymer, but it is also influenced by overlapping with the minor diffraction peaks of the sepiolite.

TGA Analysis. The thermal properties of neat RAX and RAX-sepiolite films were studied using TGA under nitrogen atmosphere. Panels A and B in Figure 8 show the typical TGA
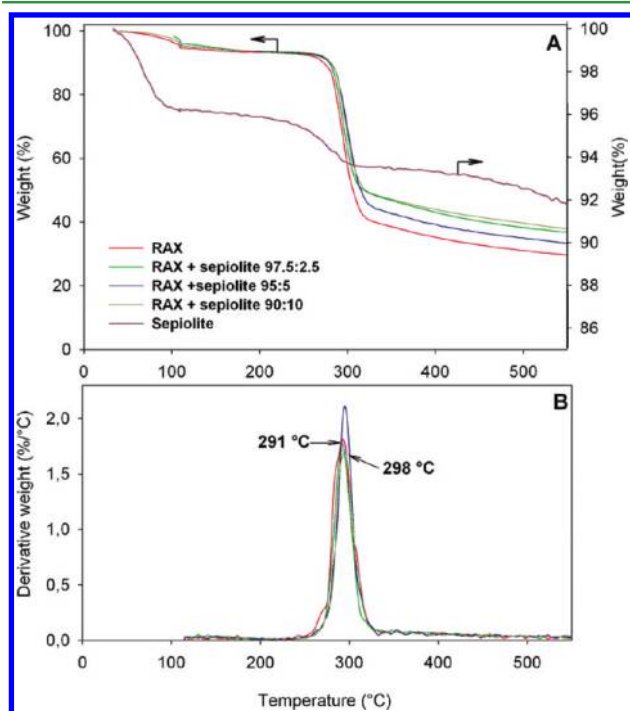
Figure 8. (A) TGA and (B) DTGA results for sepiolite, arabinoxylan (RAX), sepiolite, and composites of RAX and sepiolite in the temperature ranges 36–550 °C and 110–550 °C, respectively.

and DTGA curves for RAX, RAX-sepiolite films and sepiolite powder. Sepiolite showed a weight loss of 11.1% in the temperature range 36–900 °C (the temperature range of 36–550 °C is shown in Figure 8). Sepiolite loses zeolitic and structural water when it is heated and this is followed by loss of octahedrally coordinated hydroxyl groups (internal Mg-OH) in a four-step process with eventual collapse of the crystal structure.[20,38] Kuang et al.[20] found that maxima for the rate of weight loss occurred at 60 °C, 260 °C, 510 °C and 800–830 °C and, except for the last two, these changes are shown in Figure 8A, representing the loss of zeolitic water, structural water in two stages, and Mg-OH dehydroxylation, respectively. In Figure 8A, initial weight losses of approximately 5% are attributable to the release of water. As shown, the arabinoxylan in the RAX and composite film samples started to decompose at ~260 °C. Slight differences in maximum weight loss temperatures (T_{max}) were observed in the DTGA. For example, RAX showed a T_{max} at 291 °C, whereas T_{max} for the composite films containing 2.5, 5, and 10 wt % sepiolite were found at 295, 297, and 298 °C, respectively. A shift in T_{max} is commonly observed during thermal analysis of clay-biopolymer films. In one case, a similar temperature increase was found for starch-sepiolite composites in which the T_{max} temperature increased 3 °C at 3 wt % sepiolite addition and 8 °C at 6 wt % sepiolite addition.[12] Addition of layered nanoclays, such as MMT, has also been shown to increase degradation temperatures and in these cases the clay is thought to form an inorganic network, which act as a gas transport barrier, thereby hindering the diffusion of pyrolysis gases.[40] As a case in point, Ünlü et al.[14] cast xylan films from corn cob with MMT addition and studied the thermal behavior of such films. A T_{max} of 284 °C was found for neat xylan but this increased to 303 °C with an addition of 2 g/mL MMT to 7.8×10^{-5} g/ml xylan. It seems reasonable to assume that the fibrous sepiolite would not so easily form a tortuous path to hinder the path of pyrolysis gases and, as a result, the increases in T_{max} are less significant (Figure 8B).

Tensile Testing. The effect of sepiolite addition on RAX film mechanical properties was examined by tensile testing. The efficiency of plasticization using mPEG addition was also studied. Neat arabinoxylan films without plasticizer addition showed a tensile strength (stress at break) of 42.5 MPa, which is similar to, but slightly lower than, values reported previously for this material. For example, Höije et al.[35] and Stevanic et al.[30] measured tensile strengths of 52.4 and 58 MPa respectively for rye arabinoxylan at the same RH, but at a slightly higher temperature in the work of Stevanic et al. Addition of sepiolite resulted in a very significant increase in film strength and stiffness (Table 1). As an example, addition of 2.5 wt % sepiolite to RAX gave an increase in Young's modulus from 2.3 to 3.9 GPa and an increase in tensile strength from 42.5 to 73.6 MPa. Further addition of sepiolite showed only a minor additional increase in the Young's modulus values. In the case of the tensile strength, although there was no significant difference between the mean values determined for films with 2.5 or 10 wt % sepiolite, there was a significantly lower mean value recorded for films with 5 wt % sepiolite. This particular finding is contrary to expectation and a detailed explanation must await further research. In general, it may be said that the nonplasticized films containing sepiolite had tensile strength values in the order of 70 MPa. No statistically significant differences were detectable in the strain at break values of the neat RAX and RAX-sepiolite composites without plasticizer addition.

Table 1. Young's Modulus, Strain at Break, and Tensile Strength of Rye Arabinoxylan (RAX) and RAX-Sepiolite Composite Films[a]

sample	Young's modulus (GPa)	strain at break (%)	tensile strength (MPa)
RAX-sepiolite 90:10	4.3 ± 0.1 A	5.0 ± 0.8 C	73.7 ± 5.3 A
RAX-sepiolite 95:5	4.2 ± 0.2 A	8.1 ± 2.3 C	66.7 ± 2.3 B
RAX-sepiolite 97.5:2.5	3.9 ± 0.3 B	10.4 ± 3.1 C	73.6 ± 3.2 A
RAX	2.3 ± 0.2 C	11.9 ± 4.3 C	42.5 ± 6.5 C
RAX-sepiolite 90:10 + 30% mPEG	1.4 ± 0.1 D	26.7 ± 11.B	24.9 ± 5.1 F
RAX-sepiolite 95:5 + 30% mPEG	1.0 ± 0.2 E	33.3 ± 6.5 B	26.6 ± 2.3 EF
RAX-sepiolite 97.5:2.5 + 30% mPEG	0.8 ± 0.1 EF	44.4 ± 7.8 A	30.2 ± 6.6 DE
RAX + 30% mPEG	0.7 ± 0.1 F	42.0 ± 9.7 A	32.8 ± 7.3 D

[a]A, B, C, D, E, F: values with different superscript letters in the same column are statistically different (significance level of 0.05).

The addition of mPEG plasticizer had the expected effect of decreasing film stiffness and strength while increasing the elongation values. In the case of the RAX-sepiolite films with added mPEG, a slight increase in the Young's modulus and a decrease in the tensile strength values were observed with increasing sepiolite content. The strain at break showed values approximately four to five times higher than those of the nonplasticized films. A decrease in extensibility could be seen in films with 5 and 10 wt % sepiolite content and 30 wt % mPEG relative to unfilled RAX or RAX films with 2.5 wt % sepiolite containing the same percentage of mPEG.

The reinforcing effects of sepiolite addition have been investigated using other biopolymers such as chitosan and starch. Chivrac et al.[12] incorporated 3 and 6 wt % organo-modified sepiolite into plasticized starch and found that the Young's modulus increased by up to a factor of 2.5 relative to unfilled wheat starch. As reported, a slight decrease was found in the strain at break values with sepiolite addition and with similar clay loading as applied in our study. Similar behavior when comparing layered silicates with sepiolite was observed in gelatin films.[17] A reinforcing effect comparable to that reported here was observed and assigned to the presence of numerous silanol groups on the surface of the sepiolite fibers strongly interacting with the carbohydrate matrix. Darder et al.,[16] in their study on chitosan as the matrix, showed that sepiolite addition doubled the Young's modulus; however, this finding was obtained in the case of films containing very high sepiolite loadings. Such high sepiolite loadings (3−91 g of chitosan per 100 g of sepiolite) resulted in highly fragile films, hence strain at break was not measured and tensile strength values were not reported. With the addition of high sepiolite loadings, clay aggregation was observed in the cast films through the use of low-temperature SEM. Soler added MMT clay to arabinoxylan from barley husks and studied the reinforcing effects of MMT; however, significant effects in terms of tensile strength and Young's modulus were not seen.[41] For example, the Young's modulus and tensile strength of arabinoxylan films were 1.3 GPa and 30.8 MPa, respectively, whereas the corresponding values for films reinforced with 11 wt % MMT were 2.0 GPa and 31.6 MPa.

Given the results presented here for the reinforcing effects of sepiolite fibers, it is interesting to make comparison with the effects introduced by other fibrous nanofillers. A significant increase in the tensile strength of hemicellulose films was previously seen when using cellulose nanofibers. Since the size of nanofibrillated cellulose is in a similar range to that of sepiolite fibers and both fillers have a high aspect ratio, similar behavior may be expected. Hemicellulose-cellulose nano-composite mechanical properties are summarized in Table 2.

Table 2. Mechanical Properties of Xylan-Cellulose Nanocomposite Films

sample[a]	filler loading (wt %)	ref	Young's modulus (GPa)	strain at break (%)	tensile strength (MPa)
RAX	0	34	2.5 ± 0.4	8.1 ± 3.3	58 ± 11
RAX + BC	15		3.2 ± 0.5	3.3 ± 0.6	53 ± 7
AX[b]	0	42	0.7 ± 0.1	3.4 ± 0.2	11.9 ± 0.9
AX + NFC[b]	20		3.4 ± 0.1	1.4 ± 0.1	39.5 ± 2.2
X[c]	0	43		~22	~2.2
X + SW[c]	10			~23	~5.9

[a]RAX = rye arabinoxylan, BC = bacterial cellulose, AX = arabinoxylan, NFC = nanofibrillated cellulose, X = xylan from oat spelts, SW = sulfonated cellulose whisker. [b]Added sorbitol plasticizer, 25% (percentage based on xylan content). [c]Added sorbitol plasticizer, 50%.

Peng et al.[42] recently reported ~300% increase in tensile strength and Young's modulus with 15 wt % nanocellulose addition to bamboo arabinoxylan. In this case, nanocellulose was obtained by multihomogenization of bleached sisal pulp and had a reported aspect ratio of 50−100, based on a nanofibril diameter of 20 ± 10 nm and length >1000 nm. Such significant increases in strength and stiffness were, however, not observed when rye arabinoxylan was reinforced using bacterial nanocellulose with similar dimensions as the sepiolite applied in this study.[34] For example, the Young's modulus of arabinoxylan films showed ~30% increase in the nanocomposite with 15% bacterial nanocellulose addition.

As concluded from the FT-IR results, interaction through hydrogen bonding between the sepiolite fibers and the RAX chains can be inferred and these interactions contribute to a great increase in the stiffness of the material. It is also apparent from the results that, above a clay content of 5 wt %, fiber aggregation is more probable, which will contribute to the breakage of the films under tensile load and mean that further increases in tensile strength and Young's modulus are not likely to be detected. We may assume that the sepiolite fibers are themselves able to form a network, hence providing a reinforced composite material with superior mechanical properties compared to the neat RAX matrix. Considering the high aspect ratio of sepiolite fibers, a percolation threshold can be calculated. Since the dimensions of sepiolite fibers show a great variation in different reports,[17,23,44] a range of calculated values can be obtained for the percolation threshold between 0.6% and 3.5% (v/v) if a cylindrical sepiolite shape is assumed ($P_c = 0.7/r$, where P_c is the percolation threshold for cylindrical shaped particles and r is the aspect ratio calculated from the ratio of length and diameter of sepiolite fibers).[45] This calculation suggests that an added amount of sepiolite above the critical percolation threshold of approximately 2% (v/v) would result in highly increased strength and stiffness in the materials. As supported by the tensile data presented here, films containing sepiolite at loadings much above the estimated P_c do

not show significant further increases in tensile strength and stiffness.

Barrier Properties. Water vapor barrier properties of cast RAX-sepiolite films were studied by measuring the water vapor permeability of the films using an ASTM method. The measured values were 2.6 ± 0.3, 2.5 ± 0.0, 3.3 ± 0.4, and 3.1 ± 0.3 (g mm/(kPa m^2 day)) for the RAX, RAX + sepiolite 97.5:2.5, 95:5, and 90:10 films, respectively. These data show that sepiolite addition up to 10 wt % had no significant influence on water vapor permeability. Even though sepiolite might theoretically create a slightly longer and more difficult path for water molecules to diffuse through the films, sepiolite fibers are hydrophilic and embedded into a hydrophilic matrix with poor water vapor barrier properties. Hence, a positive effect in terms of reduced water vapor permeability is not seen. Further, the barrier effect commonly noted when plate-like clays are well dispersed in biopolymer films is not observed here, which is consistent with the different fibrous morphology of sepiolite and a lower probability that water vapor permeability will be reduced through a tortuous path effect.[46] WVP values measured for the unfilled RAX reference film were lower or in the same range as values reported previously for nonplasticized arabinoxylan films extracted from corn hulls and bran.[7,47]

The effect of sepiolite addition on RAX film oxygen permeability was studied and the results are summarized in Table 3. RAX films showed low permeability values, between 0

Table 3. Oxygen Transmission Rate (OTR) and Oxygen Permeability (OP) of Neat Rye Arabinoxylan (RAX) and RAX-Sepiolite Composite Films at 50% Relative Humidity and 23 °C[a]

type of film	OTR (mL/(m^2 day))	OP (cm^3 μm/(m^2 day kPa))
RAX	0.58–0.70	0.15–0.22
RAX-sepiolite 97.5:2.5	0.80–1.41	0.22–0.54
RAX-sepiolite 95:5	0.20–0.74	0.10–0.26
RAX-sepiolite 90:10[b]	0.69	0.19

[a]Values obtained from two measurements. [b]Only one successful measurement could be made from the samples, because of leaking as a result of defects on the film surface.

and 1 cm^3 μm/(m^2 day kPa). Low OP values were expected since hemicellulose films have proven to be excellent oxygen barriers, with values in the range of 0.16–3.2 cm^3 μm/(m^2 day kPa) reported for similar hemicellulose film types.[1,2,39] In this case, as with water vapor, sepiolite addition had no significant effect on oxygen permeability and, as above, the lack of a tortuous path effect when using a fibrous clay as additive may provide an explanation for these findings.

CONCLUSIONS

Transparent or semitransparent rye arabinoxylan (RAX) films containing 2.5–10 wt % sepiolite were cast from aqueous suspensions and characterized by various physical methods. FT-IR spectroscopy provided some evidence for hydrogen bonding between sepiolite and the RAX matrix. Strong interfacial bonding between sepiolite and the RAX matrix was illustrated by scanning electron microscopy and the good distribution of the clay was also shown using EDX imaging. Mechanical testing revealed very significant increases in the Young's modulus and tensile strength as a result of sepiolite addition, which exceeded

previously reported values for xylan/nanocellulose or xylan/MMT films. However, unlike layered nanoclays, addition of sepiolite fibers did not reduce the water vapor or oxygen permeability of RAX films and therefore other steps would need to be introduced in order to obtain higher gas barrier properties for specific applications.

AUTHOR INFORMATION

Corresponding Author
*Corresponding author. E-mail: dapl@kt.dtu.dk. Tel.:+45 4525-6813.

Notes
The authors declare no competing financial interest.

REFERENCES

(1) Gröndahl, M.; Gatenholm, P. In *Materials, Chemicals, and Energy from Forest Biomass*; Argyropoulos, D. S., Ed.; ACS Symposium Series, OUP; American Chemical Society: Washington, D.C., 2007; Vol. *954*, p 137.

(2) Mikkonen, K. S.; Heikkinen, S.; Soovre, A.; Peura, M.; Serimaa, R.; Talja, R. A.; Helén, H.; Hyvönen, L.; Tenkanen, M. *J. Appl. Polym. Sci.* **2009**, *114*, 457–466.

(3) Zhang, Y.; Pitkänen, L.; Douglade, J.; Tenkanen, M.; Remond, C.; Joly, C. *Carbohydr. Polym.* **2011**, *86*, 852–859.

(4) Hansen, N. M. L.; Plackett, D. *Biomacromolecules* **2008**, *9*, 1493–1505.

(5) Ebringerová, A.; Heinze, T. *Macromol. Rapid Commun.* **2000**, *21*, 542–556.

(6) Sternemalm, E.; Höije, A.; Gatenholm, P. *Carbohydr. Res.* **2008**, *343*, 753–757.

(7) Zhang, P.; Whistler, R. L. *J. Appl. Polym. Sci.* **2004**, *93*, 2896–2902.

(8) Ibn Yaich, A.; Edlund, U.; Albertsson, A. *Biomacromolecules* **2012**, *13*, 466–473.

(9) Mikkonen, K. S.; Heikkilä, M. I.; Willför, S. M.; Tenkanen, M. *Int. J. Polym. Sci.* **2012**, *2012*, 1–8.

(10) Saxena, A.; Elder, T. J.; Ragauskas, A. J. *Carbohydr. Polym.* **2011**, *84*, 1371–1377.

(11) Tartaglione, G.; Tabuani, D.; Camino, G.; Moisio, M. *Compos. Sci. Technol.* **2008**, *68*, 451–460.

(12) Chivrac, F.; Pollet, E.; Schmutz, M.; Avérous, L. *Carbohydr. Polym.* **2010**, *80*, 145–153.

(13) Viota, J. L.; Lopez-Viota, M.; Saake, B.; Stana-Kleinschek, K.; Delgado, A. V. *J. Colloid Interface Sci.* **2010**, *347*, 74–78.

(14) Ünlü, C. H.; Günister, E.; Atici, O. *Carbohydr. Polym.* **2009**, *6*, 585–592.

(15) Galan, E. *Clay Miner.* **1996**, *31*, 443–453.

(16) Darder, M.; López-Blanco, M.; Aranda, P.; Ruiz-Hitzky, E.; Aznar, A. J.; Bravo, J. *Chem. Mater.* **2006**, *18*, 1602–1610.

(17) Fernandes, F. M.; Manjubala, I.; Ruiz-Hitzky, E. *Phys. Chem. Chem. Phys.* **2011**, *13*, 4901–4910.

(18) Fukushima, K.; Tabuani, D.; Camino, G. *Mater. Sci. Eng., C* **2009**, *29*, 1433–1441.

(19) Olmo, N.; Lizarbe, M. A.; Gavilanes, J. G. *Biomaterials* **1987**, *8*, 67–69.

(20) Kuang, W.; Facey, G. A.; Detellier, C.; Casal, B.; Serratosa, J. M.; Ruiz-Hitzky, E. *Chem. Mater.* **2003**, *15*, 4956–4967.

(21) Sakizci, M.; Erdogan Alver, B.; Yörükogullari, E. *J. Therm. Anal. Calorim.* **2011**, *103*, 435−441.

(22) Esteban-Cubillo, A.; Pina-Zapardiel, R.; Moya, J. S.; Barba, M. F.; Pecharromán, C. *J. Eur. Ceram. Soc.* **2008**, *28*, 1763−1768.

(23) Bilotti, E.; Fischer, H. R.; Peijs, T. *J. Appl. Polym. Sci.* **2008**, *107*, 1116−1123.

(24) Karakashev, S. I.; Ozdemir, O.; Hampton, M. A.; Nguyen, A. V. *Colloids Surf., A* **2011**, *382*, 132−138.

(25) Harris, J. M.; Chess, R. B. *Nat. Rev. Drug Discov.* **2003**, *2*, 214−221.

(26) Siró, I.; Plackett, D.; Hedenqvist, M.; Ankerfors, M.; Lindström, T. *J. Appl. Polym. Sci.* **2011**, *119*, 2652−2660.

(27) *ASTM D882-09 Standard Test Method for Tensile Properties of Thin Plastic Sheeting*; ASTM International: West Conshohocken, PA, 2009.

(28) *ASTM E96/E96M−05 Standard Test Methods for Water Vapor Transmittance of Materials*; ASTM International: West Conshohocken, PA, 2005.

(29) Mikkonen, K. S.; Heikkilä, M. I.; Helén, H.; Hyvönen, L.; Tenkanen, M. *Carbohydr. Polym.* **2010**, *79*, 1107−1112.

(30) Gennadios, A.; Weller, C. L.; Gooding, C. H. *J. Food Eng.* **1994**, *21*, 395−409.

(31) Robertson, J. A.; Faulds, C. B.; Smith, A. C.; Waldron, K. W. *J. Agric. Food Chem.* **2008**, *56*, 1720−1726.

(32) Li, Y.; Jiang, Y.; Liu, F.; Ren, F.; Zhao, G.; Leng, X. *Food Hydrocolloids* **2011**, *25*, 1098−1104.

(33) Rhim, J. *Carbohydr. Polym.* **2011**, *86*, 691−699.

(34) Stevanic, J. S.; Joly, C.; Mikkonen, K. S.; Pirkkalainen, K.; Serimaa, R.; Rémond, C.; Toriz, G.; Gatenholm, P.; Tenkanen, M.; Salmén, L. *J. Appl. Polym. Sci.* **2011**, *122*, 1030−1039.

(35) Buslov, D. K.; Kaputski, F. N.; Sushko, N. I.; Torgashev, V. I.; Solov'eva, L. V.; Tsarenkov, V. M.; Zubets, O. V.; Larchenko, L. V. *J. Appl. Spectrosc.* **2009**, *76*, 801−805.

(36) Robert, P.; Marquis, M.; Barron, C.; Guillon, F.; Saulnier, L. *J. Agric. Food Chem.* **2005**, *53*, 7014−7018.

(37) Kacuráková, M.; Wellner, N.; Ebringerová, A.; Hromádková, Z.; Wilson, R. H.; Belton, P. S. *Food Hydrocolloids* **1999**, *13*, 35−41.

(38) Perraki, T.; Orfanoudaki, A. *J. Therm. Anal. Calorim.* **2008**, *91*, 589−593.

(39) Höije, A.; Sternemalm, E.; Heikkinen, S.; Tenkanen, M.; Gatenholm, P. *Biomacromolecules* **2008**, *9*, 2042−2047.

(40) Sinha Ray, S.; Okamoto, M. *Prog. Polym. Sci.* **2003**, *28*, 1539−1641.

(41) Soler, C. A. B. *Preparation and Characterization of Arabinoxylan-Montmorillonite Nanocomposites*; Chalmers Univeristy of Technology: Göteborg, Sweden, 2008.

(42) Peng, X.; Ren, J.; Zhong, L.; Sun, R. *Biomacromolecules* **2011**, *12*, 3321−3329.

(43) Saxena, A.; Elder, T. J.; Pan, S.; Ragauskas, A. J. *Composites, Part B* **2009**, *40*, 727−730.

(44) Tunc, S.; Duman, O.; Cetinkaya, A. *Colloids Surf., A* **2011**, *377*, 123−129.

(45) Yudin, V. E.; Otaigbe, J. U.; Svetlichnyi, V. M.; Korytkova, E. N.; Almjasheva, O. V.; Gusarov, V. V. *eXPRESS Polym. Lett.* **2008**, *2*, 485−493.

(46) Grunlan, J. C.; Grigorian, A.; Hamilton, C. B.; Mehrabi, A. R. *J. Appl. Polym. Sci.* **2004**, *93*, 1102−1109.

(47) Peroval, C.; Debeaufort, F.; Despre, D.; Voilley, A. *J. Agric. Food Chem.* **2002**, *50*, 3977−3983.